

# Heater induced thermal effects on the LTP dynamics

**F Gibert<sup>1,3</sup>, A Lobo<sup>1,2</sup>, M Diaz-Aguiló<sup>1,4</sup>, I Mateos<sup>1</sup>, M Nofrarias<sup>5</sup>, J Sanjuán<sup>6</sup>, A Conchillo<sup>1,2</sup>, L Gesa<sup>1,2</sup> and I Lloro<sup>1,2</sup>**

<sup>1</sup> Institut d'Estudis Espacials de Catalunya (IEEC), Barcelona, Spain

<sup>2</sup> Institut de Ciències de l'Espai (CSIC-IEEC), Barcelona, Spain

<sup>3</sup> Escola Tècnica Superior d'Enginyeries Industrial i Aeronàutica de Terrassa (ETSEIAT), Universitat Politècnica de Catalunya (UPC), Terrassa, Spain

<sup>4</sup> Escola Politècnica Superior de Castelldefels (EPSC), Universitat Politècnica de Catalunya (UPC), Castelldefels, Spain

<sup>5</sup> Max-Planck-Institut für Gravitationsphysik, Albert Einstein Institut (AEI), Hannover, Germany

<sup>6</sup> Department of Physics, University of Florida, Gainesville, FL, United States

E-mail: [gibert@ieec.cat](mailto:gibert@ieec.cat)

**Abstract.** The STOC (Science and Technology Operations Centre) simulator of the LPF (LISA PathFinder) mission is intended to provide a validation tool for the mission operations tele-commanding chain, as well as for a deeper understanding of the underlying physical processes happening in the LTP (LISA Technology Package). Amongst the different physical effects that will appear onboard, temperature fluctuations in the Electrode Housing (EH) could generate disturbances on the interferometer (IFO) readouts, therefore they must be known and controlled. In this article we report on the latest progress in the analysis at IEEC of the LTP response to thermal signals injected by means of heaters. More specifically, we determine the transfer functions relating heat input signals to forces on the Test Masses (TMs) in the LTP frequency band, from 1 mHz to 30 mHz. A complete thermal model of the entire LPF spacecraft plus payload, elaborated and maintained at European Space Technology Center (ESTEC), was used to obtain temperature distributions in response to heat inputs at prescribed spots (heaters), which are later processed to calculate the associated dynamical effects on the Test Masses.

## 1. Introduction

Undesired temperature fluctuations around the TMs and in other points of LTP have been identified as disturbances that could alter IFO readouts. In order to keep them controlled, a set of experiments, gathered in the Experiment Master Plan (EMP), are planned to be conducted onboard LPF so the effects can be measured and later use the results to assess the weight of temperature noise in the global noise budget.

All this involves the necessity of modelling and simulating the different thermal effects. To achieve this goal, the STOC simulator of LPF, that is aimed to recreate the behavior of the spacecraft through its main operational phases, must include them.

In this article, we focus only on the consequences of thermal effects at EH due to the activation of the different Data and Diagnostics System (DDS) heaters following the plans from the EMP. Specifically, in the following a description of the process considered to determine forces acting on TMs is explained, as well as the simulations of the heat input in the system. In the last sections, results from the simulations are presented and discussed.

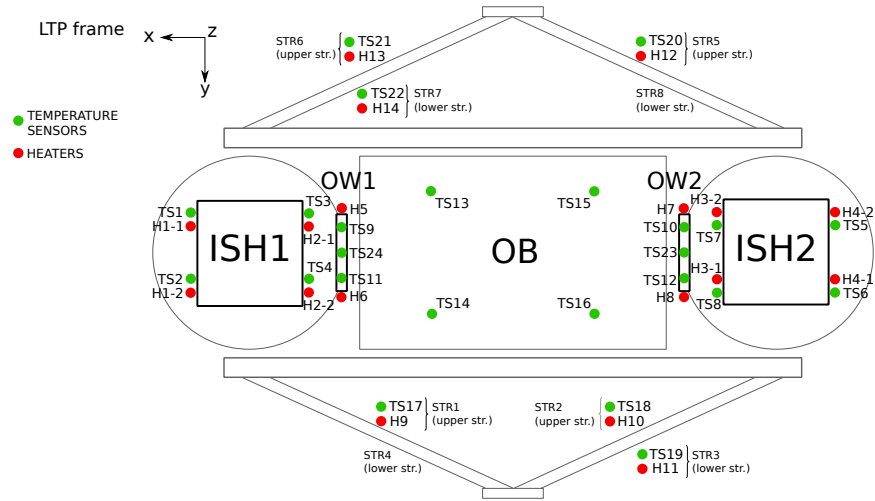


**Figure 1.** Figure caption for first of two sided figures.

## 2. Basis

### 2.1. General layout of DDS thermal items

The DDS thermal items are composed by 18 *physical* heaters and 24 temperature sensors [1]. The general scheme of the distribution and nomenclature is shown in Figure 1, and a scheme only of the EH is presented in Figure 2. Figure 3 shows a global picture of the LTP.

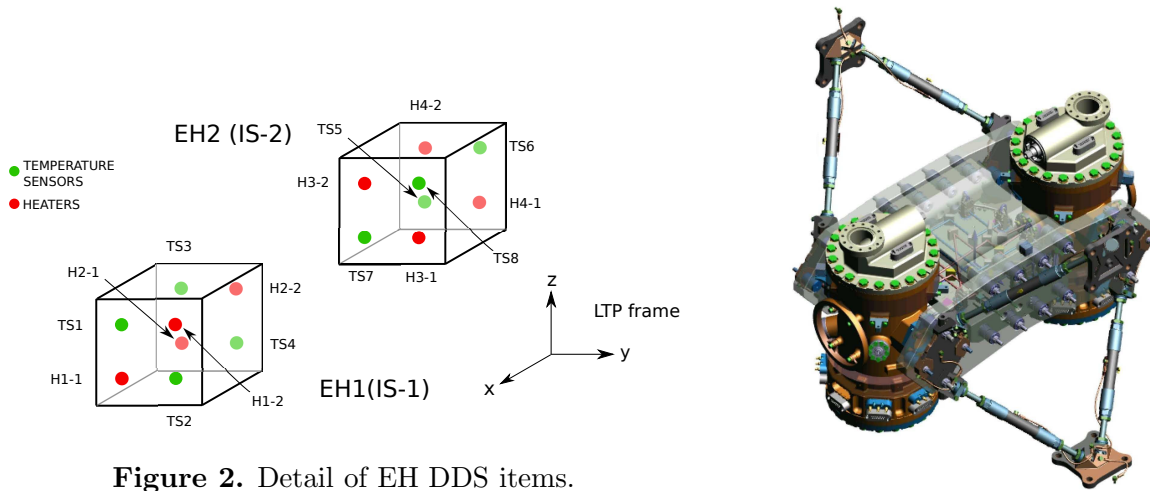


**Figure 2.** Detail of EH DDS items.

**Figure 3.** General picture of the LTP.

### 2.2. EMP thermal calibration description

The Experiment Master Plan (EMP) thermal calibration aims to characterize the consequences of asymmetric temperature fluctuations happening in the LTP. Experiments consist of applying well-defined heat loads at specific points of LTP and observe induced temperature variations at particular points in order to see which are their consequences. Their ultimate goal is to calibrate these effects so that the temperature noise can eventually be subtracted from the IFO readout.

Thermal EMP exercises can be divided into three groups, depending on the main focus of the exercise and the heaters that are being activated:

- (a) Determination of forces and torques on the TMs due to EH heaters activation.
- (b) Determination of IFO phase shifts due to Optical Window (OW) heaters activation.
- (c) Determination of IFO phase shifts due to Suspension Struts (STR) heaters activation.

Dynamic effects from exercises performed at (a) come as a result of the existence of different thermal effects appearing in the EH environment - see Section 2.4-, while experiments from (b) and (c) are aimed to analyze thermoelastic effects caused by heating the OWs and creating stresses on the Optical Bench, respectively, and should not interfere with the TMs dynamics.

The specific input power sequences are described in Table 1 [2, 3]. They are intended to generate enough *disturbance* in specific spots so the IFO can detect their presence. However, they may present side effects that must be also studied, particularly in the dynamics of the TM during exercises (b) and (c), due to the amount of total heat applied.

**Table 1.** Input signals for each experiment. Experiments from (a) apply heat to pairs of EH heaters from same face of a TM alternatively, while in ones from (b) and (c) simple pulse series are applied to single a heater each time.

Experiment	Power	Period	Duty cycle	Duration
(a) EH	1-80 mW	2000 s	50%	4000 s
(b) OW	0.1-1 W	1000 s	5%	5000 s
(c) STR	0.5-2 W	2500 s	4%	7500 s

### 2.3. Signal requirements

LPF main noise requirements are given as a spectral density of noise by [5]

$$S_{\Delta a, \text{LPF}}^{1/2}(\omega) \leq 3 \times 10^{-14} \left[ 1 + \left( \frac{\omega/2\pi}{3 \text{ mHz}} \right)^2 \right] \text{ m s}^{-2} \text{ Hz}^{-1/2} \quad (1)$$

in the band from 1mHz to 30 mHz. Considering that the mass of each TM is 1.96 kg [4], Equation 1 consequent conversion to force requirement is expressed with

$$S_{\Delta F, \text{LPF}}^{1/2}(\omega) \leq 5.9 \times 10^{-14} \left[ 1 + \left( \frac{\omega/2\pi}{3 \text{ mHz}} \right)^2 \right] \text{ N Hz}^{-1/2} \quad (2)$$

On the other hand, the SNR requirement to detect thermally created signals in the inertial sensor (IS) with the IFO is  $SNR \geq 50$  [5], and it is obtained, considering a force signal  $F(t)$ , as

$$(SNR)^2 = \frac{2}{\pi} \int_{BW} \frac{|\tilde{F}(w)|^2}{S_{\Delta F, \text{LPF}}(w)} dw \quad (3)$$

where  $\tilde{F}(w)$  is the Fourier Transform of the force signal  $F(t)$ .

### 2.4. Thermal effects

Temperature differences across the TMs environment can produce differential pressures that turn to net forces and torques on the TMs. Three different thermal effects have been identified as mechanisms responsible of these quantities [6]:

*2.4.1. Radiation pressure effect* It is based on the temperature-dependence of the radiation emitted by a heated surface. The pressure generated is expressed as:

$$P_{\text{rdn}} = \frac{8}{3} \frac{\sigma T^3}{c} \Delta T \text{ Pa} \quad (4)$$

where  $\sigma$  is the Stefan-Boltzmann constant,  $c$  is the speed of light,  $T$  is the absolute temperature and  $\Delta T$  is the temperature difference between two surfaces.

*2.4.2. Radiometer effect* It appears in rarified atmospheres where the particles have a mean free path much longer than the distance between the two surfaces. The consequent pressure is represented here as:

$$P_{\text{rmt}} = \frac{1}{4} \frac{p}{T} \Delta T \text{ Pa} \quad (5)$$

where  $p$  stands for the remaining gas static pressure.  $T$  and  $\Delta T$  have same meanings as in Equation 4.

*2.4.3. Outgassing effect* A third thermal effect with poorly known consequences, the outgassing effect could appear. Models of this effect made so far are not accurate enough, therefore it will not be considered here.

### 3. Procedure

The procedure can be split in two parts, the first one concerning all the operations related with the data from the thermal model and the following fit that allows to calculate the temperature distribution, and the second one related with the force modelling.

#### 3.1. Thermal model

The thermal model used to simulate the thermal behaviour of the different parts under analysis is the current ESATAN version that can be found at ESTEC. Samples of transfer functions containing the temperature response in a node after applying heat into another can be directly determined by the ESATAN program.

A set of specific thermal nodes concerning the temperature sensor nodes and the nodes of the different electrodes in the EH were selected as representative of the temperature distribution response [7], and their transfer function samples were provided by ESTEC. Data was fitted using LTP Data Analysis Tool software in order to get analytic expressions for each *node to node* relation.

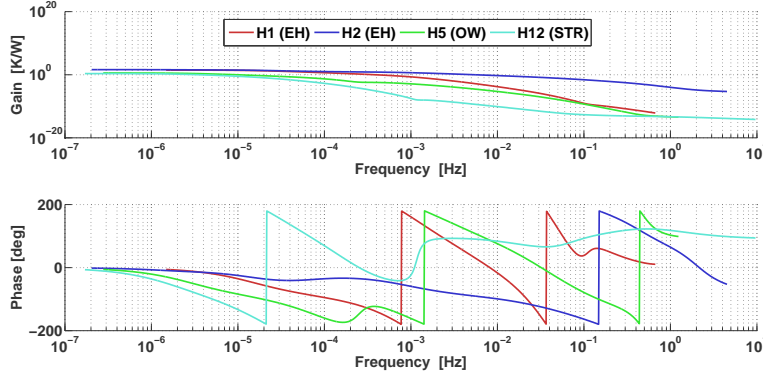
Additionally to these transfer functions, specific thermal behavior for the heaters modelling their thermal resistance was considered also [8], and it was combined with the initial transfer functions so as to get a more approximate model of the case. With the definitive relation, time response of temperature at different points due to the activation of different heaters were directly determined.

Figure 4 shows a group of Bode Plots as an example of the different transfer functions obtained.

#### 3.2. Modelling forces

Considering the geometry of the case and assuming that only the faces containing EH heaters are relevant for the calculation of forces along the X axis, it is possible to express the resulting force with Equation 6.

$$F_X = F_{\text{rdn}} + F_{\text{rmt}} = \frac{8}{3} \frac{\epsilon_{ij} A \sigma T_0^3}{c} \Delta T_{AB} + \frac{1}{4} \frac{Ap}{T_0} \Delta T_{AB} = \left( \frac{8}{3} \frac{\epsilon_{ij} A \sigma T_0^3}{c} + \frac{1}{4} \frac{Ap}{T_0} \right) \Delta T_{AB} \text{ N} \quad (6)$$



**Figure 4.** Bode plots of the temperature response at temperature sensor TS3 location (-X face of EH1). The different heaters considered are H1, H2, H5 and H12.

where  $A$  is the area where the pressure is applied and  $\epsilon_{ij}$  is the view factor between two EH-TM surfaces.

Replacing with the nominal values of the case [4] and considering a view factor  $\epsilon_{ij} = 0.683$ , the resulting temporal *force-temperature* relation states  $F_X(t) = 36.4\Delta T(t)$  pN, where  $\Delta T(t)$  is the temperature difference between both X inner faces of a single EH at time  $t$ .

## 4. Results

### 4.1. EH heaters

Figures 5 and 6 present the time response of the temperature gradient and force in X axis with a power input of 10mW. The higher amplitude of the first peak in Figure 6 is created due to the initial *cold* environment in the EH. Therefore, the total force applied will tend to be assymetrical.

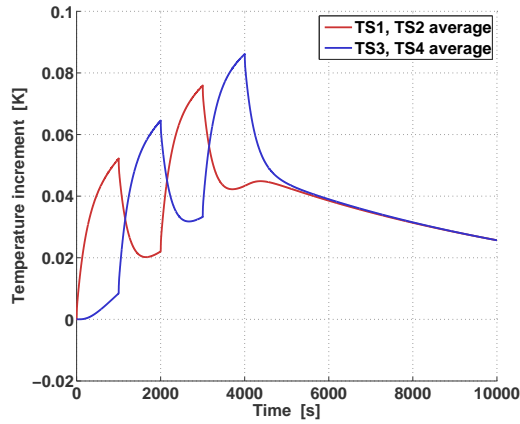


**Figure 5.** Absolute temperature increment values for each side of TM-1 along exercise (a).

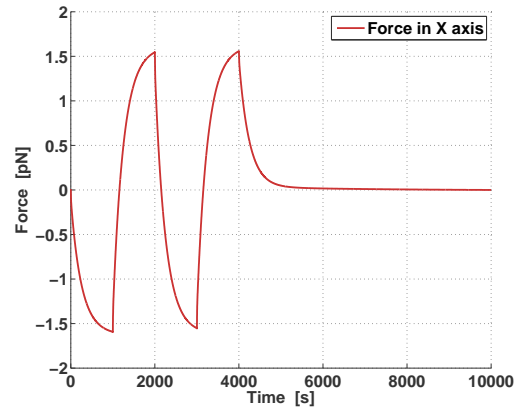


**Figure 6.** Force in X axis on TM-1 along exercise (a).

The SNR obtained from this exercise is of about 116, considering an integration time of 50,000 seconds, what meets the requirement.

### 4.2. Side effects on EH

Exercise (b) produces a SNR due to forces in EH of  $\sim 0.93$  when a power of 0.2 W is applied, while exercise (c) gets a SNR of  $\sim 0.02$  with a power of 2 W. In both cases, an integration time of 100,000 seconds was considered.

### 4.3. Transient times

The transient time length is also of great interest, because it sets the required relaxation time between different exercises and the total length of the experiment. Taking into account that considerable amounts of power are applied in some cases, it should be expected that long periods of time would be required between different exercises.

For example, referring to exercise (a), the time that it takes for the EH to cool back to 10% of the maximum absolute temperature reached is about 22,000 s, while the time that it needs to recover to 10% of maximum differential temperature is about 4,600 s.

However, for the cases of exercises (b) and (c) it is not that clear, as the hottest points are reached far from the EH. Relaxation times of these exercises can easily be a matter of days, although they vary with the distance of the heater to each EH and the total amount of heat applied.

## 5. Conclusions

Thermal response of the EH thermistors to the activation of the different LTP heaters already analysed. Analysis results so far point to:

- EH heaters activation parameters produce forces on the TM which are 100 or more times the background noise.
- Depending on the applied power, OW heating can be sensed in the EH with SNR around 1.
- STR heating does not cause noticeable effects at TM.

It is important to remark that the current power margins allow a set of possible heat inputs that in some cases could involve quite long relaxation times. In order to assess them appropriately, more detailed analysis of each case should be done, including thermoelastic effects, which are beyond the scope of this paper. Further work is still required, specifically in detailing a more accurate temperature distribution around the TMs, that will be obtained from ESATAN-provided electrode temperatures. This more detailed data will have to be correlated with the EH temperature sensor readouts.

Finally, forces in the Y and Z axes of the EH must, and will be studied, as well as torques generated from the same sources, although their impact is not expected to affect too much. Work is currently underway on these matters.

## Acknowledgments

This study has been supported by MICINN-CSIC contract ESP2007-61712. FG also acknowledges a grant from the project *Hibridació d'assignatures d'elevat contingut tecnològic com a prova pilot per als nous plans d'estudis de Grau i Màster de la titulació d'Enginyeria Aeronàutica a l'ETSEIAT*, from Departament de Projectes d'Enginyeria at ETSEIAT-UPC.

## References

- [1] G Kahl 2007, *DDS Subsystem Specification*, Report S2-ASD-RS-2004, v4.4.
- [2] M Nofrarias *et al* 2009, *Thermal experiments on board LTP*, Report S2-IEC-TN-3042, v1.1.
- [3] M Nofrarias 2006, *DDS heaters characterisation*, Report S2-IEC-TN-3025, v1.1.
- [4] N Brandt *et al* 2007, *Experiment Performance Budget*, Report S2-ASD-RP-3036, v2.
- [5] S Vitale *et al* 2005, *Science Requirements and Top-Level Architecture Definition for the LISA Technology Package (LTP) on Board LISA Pathfinder(SMART2)*, Report LTPA-UTN-ScrD, Iss3-Rev1.
- [6] M Nofrarias 2007, *Thermal diagnostic in the LISA technology package experiment*, Chapter 2. PhD thesis, Barcelona.
- [7] A Lobo 2010, *LTP thermal response to periodic signals injected by heaters*, Report S2-IEC-TN-3059, v1.
- [8] J Sanjuán 2009, *Development and validation of the thermal diagnostics instrumentation in LISA Pathfinder*, Appendix B. PhD thesis, Barcelona.